ELSEVIER

Biophysical Chemistry 113 (2005) 255–263

Biophysical Chemistry

www.elsevier.com/locate/bpc

The effect of overhanging nucleotides on fluorescence properties of hybridising oligonucleotides labelled with Alexa-488 and FAM fluorophores

J.E. Noble[a], L. Wang[b,*], K.D. Cole[b], A.K. Gaigalas[b]

[a]*Biotechnology Group, Quality of Life Division, National Physical Laboratory, Queens Road, Teddington, Middlesex, TW11 0LW, United Kingdom*
[b]*Biotechnology Division, National Institute of Standards and Technology (NIST), 100 Bureau Drive, Stop 8312, Gaithersburg, MD 20899-8312, USA*

Received in revised form 22 September 2004; accepted 22 September 2004
Available online 18 October 2004

Abstract

In order to rationally select and design probes for real-time PCR, we have determined the influence of the overhang region of the complementary strand on the resulting fluorescence from a hybridising probe. A series of target oligonucleotides, each with a unique 3′ overhang (4 bases), was hybridised to either 5′ fluorescein (FAM)- or Alexa-488-labelled probes, and the changes in fluorescence properties were monitored. We found that the number of guanine bases in the overhang region of the target oligonucleotides was proportional to the amount of fluorescence quenching observed for both the FAM and Alexa-488 dyes. FAM appeared to be more sensitive to guanine-induced quenching with three and four guanine bases resulting in greater than a twofold decrease in the quantum yield of the fluorophore compared to the no-overhang target. In addition, we found that adenine bases caused fluorescence quenching of the Alexa-488-labelled probe, whereas the FAM-labelled probe appeared insensitive. The quenching data, generated with the steady-state fluorescence measurements, displayed a linear correlation with that obtained using a fluorescent thermal cycler, suggesting the applicability to real-time PCR measurements. Anisotropy data from the series of duplexes correlated with the fluorescence quantum yield, suggesting that quenching was accompanied by increased dye mobility.
Published by Elsevier B.V.

Keywords: Nucleotides; Alexa-488; FAM

1. Introduction

Fluorescent labelling of oligonucleotide probes has facilitated the detection of specific genes, DNA, or RNA constructs in biological samples using various detection strategies. Fluorescence has many advantages over other detection methods including sensitivity, safety, and flexibility. The detection of specific DNA and RNA molecules through hybridisation to a labelled complementary probe is employed in many assays including FISH [1], mircroarrays [2], and real-time PCR [3]. Oligonucleotides can be labelled either noncovalently or covalently at specific sites of the oligos. Both covalent and noncovalent attachment display environmentally sensitive fluorescence, dependent of the attachment site and surrounding nucleotide sequence.

When covalently bound to oligonucleotides, the fluorescence from fluorescein (FAM) [4,5] and many other fluorophores [6] has been shown to be dependent of their microenvironment. Guanine and guanosine have good electron-donating properties and cause fluorescence quenching of many fluorescent dyes that are commonly employed in biological applications [6,7]. The quenching mechanisms are thought to involve photo-induced electron transfer from the nucleotide to the singlet excited state of the fluorophore. Other mechanisms operating in parallel include hydrophobic interactions and proton coupled transfer which allow endergonic electron transfer to operate [7].

* Corresponding author. Tel.: +1 301 975 2447; fax: +1 301 975 5449.
E-mail address: lili.wang@nist.gov (L. Wang).

0301-4622/$ - see front matter. Published by Elsevier B.V.
doi:10.1016/j.bpc.2004.09.012

Various studies have demonstrated that probes labelled with a 5′ fluorescein (FAM) can be quenched by the presence of guanine bases in the same strand [8] and in a complementary hybridising strand [4,5]. Quenching from guanine bases in a hybridising strand can be either in the complementary region [5,6] or part of a 3′ overhang region that is adjacent to the fluorophore attachment site of the probe. The degree of quenching depended on various factors, including guanine position relative to the fluorophore attachment site, number of guanines, and the attachment site of the fluorophore in the oligonucleotide (including attachment chemistry). The change in fluorescence intensity attributed to guanine quenching has been exploited to develop novel detection assays for DNA and RNA molecules [9,10].

It would be beneficial to be able to predict, and then either avoid or make use of low quantum efficiencies of certain fluorophores because of quenching from nucleotides to maximize the detection limits and sensitivity of hybridisation-based nucleic acid assays, such as DNA microarrrays, FISH, and real-time PCR. For instance, fluorescent detection methods employing fluorescence resonance energy transfer (FRET) are especially problematic as decreases in the donor fluorescence could be due to both resonance energy transfer and quenching by the microenvironment including specific nucleotides. On the other hand, the use of molecular beacons with high guanine content in the stem region helps to decrease the initial background from the beacon itself in real-time PCR [11]. The current work is designed to generalize the sequence dependence of fluorescence and ultimately to assist the development of model DNA reference materials for standardizing real-time PCR measurements and instruments.

The majority of the research on fluorescence quenching has concentrated on the presence of quenching nucleic acid bases in either the probe strand or its complementary strand. However these probes are typically 20–50 bases in length and are significantly shorter than the target sequences that they are used to identify. This often results in a region of single stranded ‘target’ DNA that can interact with a 5′ - or 3′ -labelled fluorophore of the probe. We have studied the effect of this overhang sequence on the fluorescence of two fluorophores that are commonly used in real-time PCR experiments (Alexa-488 and FAM). A series of target oligonucleotides were synthesized with unique 3′ 4-base overhang sequences, which would be adjacent to the 5′ -labelled fluorophore and might interact with the dye molecule when hybridised to the probe. The 4-base overhang serves as a good model for target molecules analysed using real-time PCR in that significant quenching was observed in the presence of guanine bases in the overhang region, close to the fluorophore labelling nucleotide [10,12]. Changes in fluorescence upon hybridisation were detected through fluorescence intensity and anisotropy measurements. The study enables examination of the effect of overhang target sequence on fluorescence of two most popular fluorophores and provides general guidance for nucleic acid detections.

Table 1
Nomenclature and base sequences of the oligonucleotides used in this study

Annotation	Sequence
Probes	
Alexa-Probe	5′-/**Alexa-488**/TGC GCC CAT TTT TCA AGC TGC G-3′
Fl-Probe	5′-/**Fluorescein**/TGC GCC CAT TTT TCA AGC TGC G-3′
Target	
No-overhang	5′ -CGC AGC TTG AAA AAT GGG CGC A-3′
TTGT	5′ -CGC AGC TTG AAA AAT GGG CGC ATG TT-3′
TGTT	5′ -CGC AGC TTG AAA AAT GGG CGC ATT GT-3′
GTTT	5′ -CGC AGC TTG AAA AAT GGG CGC ATT TG-3′
TTTG	5′ -CGC AGC TTG AAA AAT GGG CGC AGT TT-3′
GGTT	5′ -CGC AGC TTG AAA AAT GGG CGC ATT GG-3′
TGTG	5′ -CGC AGC TTG AAA AAT GGG CGC AGT GT-3′
GTGT	5′ -CGC AGC TTG AAA AAT GGG CGC ATG TG-3′
TTGG	5′ -CGC AGC TTG AAA AAT GGG CGC AGG TT-3′
GGGT	5′ -CGC AGC TTG AAA AAT GGG CGC ATG GG-3′
TGGG	5′ -CGC AGC TTG AAA AAT GGG CGC AGG GT-3′
AAAA	5′ -CGC AGC TTG AAA AAT GGG CGC AAA AA-3′
CCCC	5′ -CGC AGC TTG AAA AAT GGG CGC ACC CC-3′
TTTT	5′ -CGC AGC TTG AAA AAT GGG CGC ATT TT-3′
GGGG	5′ -CGC AGC TTG AAA AAT GGG CGC AGG GG-3′

The ‘target’ annotation is given as the sequence of the 3′ overhang region (4 bases) read from 3′ to 5′ end. Bold font in the sequences designates a 5′ covalently bound fluorophore attached through an aminohexylphosphate linker.

2. Materials and methods

2.1. Preparation of oligonucleotides and hybridisation

All oligonucleotides were synthesized and HPLC purified by Integrated DNA Technologies (Coralville, IA).[1] The probe was labelled with a 5′ fluorescein (FAM) or Alexa-488 NHS ester by Integrated DNA Technologies, using standard phosphoramidite chemistry via an aminohexylphosphate linker. The probe sequence was derived from the genome of bacterium *Bacillus globigii* and detailed in Table 1. All sequences were analysed using MFOLD Web Server (Version 3.1) [13] to ensure that potential secondary structures did not complicate the results.

The stock solutions of both probe and target oligos were made in TE buffer (10 mM Tris–HCl pH 8.0 and 1 mM EDTA) and further dilutions were made in the hybridisation buffer (20 mM Tris–HCl pH 8.4, 50 mM KCl and 2 mM $MgCl_2$). The concentration of target oligos was determined by measuring the absorbance at 260 nm. The concentration

[1] Certain commercial equipment, instruments, and materials are identified in this paper to specify adequately the experimental procedure. In no case does such identification imply recommendation or endorsement by the National Institute of Standards and Technology, nor does it imply that the materials or equipment are necessarily the best available for the purpose.

of the fluorophore-labelled probes was determined by averaging the concentrations derived from the absorbance at 260 nm and absorbance of the respective fluorophore. The extinction coefficients employed are 75,000 M^{-1} cm^{-1} at 495 nm for FAM and 71,000 M^{-1} cm^{-1} at 494 nm for Alexa-488 fluorophore [14], respectively.

Hybridisation reactions were performed using the following protocol: 25 °C for 30 s, 90 °C for 2 min, then decreasing the temperature to 25 °C at the rate of 0.2 °C/s and incubation at 25 °C for 8 min. A molar ratio of 1 probe molecule to 1.5 target molecules was employed. We demonstrated below that complete hybridisation of the labelled probe occurred at this ratio. Hybridisation of the target and fluorophore-labelled probe was confirmed by analysing the reactions on polyacrylamide gels (10–20% Linear Gradient, 4% stacking gel, Tris–HCl buffer) from BioRad (Hercules, CA). The PCR low ladder, 20–1000 bp marker (Sigma-Aldrich, St. Louis, MO), was used to estimate the sizes of the DNA duplexes formed. Changes in the migration of the fluorescent probe were detected on the DNA gel by illumination with a 488-nm excitation source, and the size of the fragments was estimated using the GeneScan -120 LIZ Size standard from Applied Biosystems (Foster City, CA). Fluorescence measurements were performed using 100 nM of fluorophore-labelled probe and 150 nM of unlabelled target.

2.2. Steady-state fluorescence measurements

Steady-state fluorescence spectra were recorded with a SLM 8000 spectrofluorimeter from Jobin Yvon (Edison, NJ). Typically, 130-μl reaction volumes were analysed for the fluorescence steady state and anisotropy measurements (1 cm path length). Emission spectra were collected from 505 to 560 nm with excitation at 490 nm. The slits for excitation and emission monochromators were both set at 4 nm and fluorescence spectra were collected under the 'magic angle' condition. Fluorescence intensity values were derived from the 'area under the spectra' with the background value from hybridisation buffer subtracted. Relative fluorescence quantum yield was derived from the use of a fluorescein standard [NIST Standard Reference Material (SRM) 1932, Gaithersburg, MD], which was diluted to 100 nM in 0.1 M borate buffer, pH 9.1. Under these conditions the fluorescein standard gives a quantum yield of 0.93, which is equivalent to that reported in 0.01 M NaOH [15]. The general equation for the determination of quantum yields (Q) is given by Eq. (1) [16].

$$Q_u = \frac{Q_s A_s F_u \lambda_s n_u^2}{F_s A_u \lambda_u n_s^2} \quad (1)$$

where the subscripts s and u represent the fluorescein standard and unknown, respectively. The parameter A is the absorbance at the excitation wavelength (490 nm), λ is the excitation wavelength and F is the integrated area under the emission spectrum. The square of the refractive index 'n' is employed to correct for changes in the refractive properties of the solvents used for the standard and unknown samples.

The fluorescence anisotropy (r) of the hybridisation reactions was determined using Eq. (2):

$$r = \frac{(F_{VV} - GF_{VH})}{(F_{VV} + 2GF_{VH})} \quad (2)$$

where G is the correction factor for the detection system, and is calculated using the ratio F_{HV}/F_{HH}, where the subscripts V and H refer to fluorescence intensities obtained using the vertical and horizontal polarizers, respectively, in the order of excitation followed by emission.

2.3. Thermal cycler fluorescence measurements

Melting curves for all the hybridisation reactions were performed on a LightCycler from Roche Diagnostics (Indianapolis, IN). Twenty-microliter samples of hybridisation reactions with both the FAM and Alexa-488-labelled probes were prepared as described in Preparation of oligonucleotides and hybridisation. Fluorescence from these samples was detected in the green fluorescence channel (ex/em 470/530 nm) during a holding stage at 30 °C. The temperature was then increased to 95 °C at a rate of 0.1 °C/s and fluorescence was measured again during a hold step of 60 s at 95 °C. Obtaining fluorescence data at various temperatures in a sealed system allowed individual reactions to be analysed in the hybridised (30 °C) and the unhybridised (95 °C) states. The data for each fluorophore-labelled probe could therefore be normalized by the unhybridised value to facilitate the comparison of the hybridised data [5]. The intensity value during the 60-s hold step at 95 °C was relatively stable suggesting that photobleaching/thermal degradation of the fluorophore was low. The data is expressed in arbitrary fluorescence units, rather than quantum yield relative to the fluorescein standard because the fluorescent standard is only valid at room temperature, whereas the lightcycler data was acquired over a range of temperatures (30–95 °C). Where a considerable change in fluorescence intensity occurred upon melting, the melting temperature (T_m) was determined using the melting curve analysis program with the LightCycler software, which employs a polynomial background correction step. The standard deviations (S.D.) for the melting temperatures were obtained through multiple repeated experiments.

2.4. Duplex structural modelling

The structural modelling of the hybridisation products was performed using Amber molecular mechanics (MM) code contained in Hyperchem 7.5. Amber is widely used, and has provided reasonable structures for DNA [17]. The nucleic acid database in Hyperchem 7.5 was used to build the initial DNA sequence. We used only the first five base

pairs of the target-probe duplex given in Table 1. Five base pairs provided reasonable computation times, and were sufficient to preserve the duplex structure upon attachment of Alexa-488 fluorophore (as an example) and the overhang region to one end of the duplex. Alexa-488 fluorophore was attached via a six-carbon linker to the oxygen on the phosphate of the T base on the probe sequence. The MM procedure used the parameter set amber99. The atomic charges of atoms comprising Alexa-488 were computed using AM1 semi empirical code also contained in Hyperchem 7.5. These atomic charges were then used in the MM calculation. The oxygen atoms attached to the sulfur atoms in Alexa-488 were treated similarly to oxygen atoms in the phosphate group. It is expected that the chemical environment in Alexa-488 is similar to the chemical environment in nucleic acids so that the assigned atom types are reasonable for Alexa-488 fluorophore. Solvent was modelled by a distance dependent dielectric constant.

3. Results

3.1. Both the Alexa-488- and FAM-labelled probes display target-sequence-sensitive fluorescence

A series of hybridisation experiments was performed to determine the effect of the target overhang sequence on the fluorescence of a hybridising probe. Two fluorophore-labelled probes (Alexa-488 and FAM) were hybridised to a series of unlabelled target molecules listed in Table 1, differing in the sequence of their 3′ overhang region. The target sequences were analysed using MFOLD Web Server (Version 3.1) with the most stable secondary structure predicted to occur in the 'CCCC' target generating a T_m of 57.1 °C. This value is well below the T_m (~65 °C) for all of the duplexes formed with the fluorophore-labelled probes and was therefore not considered a significant problem. To confirm that hybridisation had occurred the reaction products were analysed on a polyacrylamide gel using fluorescence to visualize the migration band of the duplex, which is different from that of single-stranded labelled probe. Unhybridised (single-stranded) DNA migrated faster than the duplexes, allowing easy discrimination. We confirmed that duplex formation was essentially completed in all hybridisation reactions.

The use of the fluorescein standard for the steady-state fluorescence analysis allowed all the measurements to be compared in terms of the quantum yield of the labelled duplex. Table 2 details the quantum efficiencies for all the hybridisation reactions employing the Alexa-488- and the FAM-labelled probes. Previously, other groups have reported that both FAM and Alexa-488 fluorophores were quenched by the presence of guanine bases in the FAM-labelled strand and the complementary strand [4–6]. The quenching data for Alexa-488 fluorophore is very limited [6]. In the present study, a comparison of overhang sequences composed of homogeneous bases shows that guanine results in the largest decrease in fluorescence to 42.9% and 65.8% for FAM and Alexa-488, respectively, compared to the no-overhang duplex. To obtain the contribution of fluorescence quenching from the overhang region, we compared the fluorescence quantum yields of duplexes with overhanging bases with those without the overhang. Logically, fluorescence quenching from the complementary region of the duplexes ought to be the same for both types of duplexes with and without the overhang region. The presence of an overhang composed of four cytosines, four thymines, or four adenines resulted in a modest decrease in fluorescence for the FAM probe compared to that with no-overhang (Table 2), although the yield for four thymines as the overhang was slightly lower than those for four cytosines and four adenines. For the Alexa-488-labelled probe, however, four adenines appeared to cause a decrease in fluorescence when compared to four thymines or four cytosines that resulted in a slight increase in fluorescence with regard to that with no overhang (Table 2).

The presence of a guanine base in the 3′ overhang region of the hybridising sequence displayed the greatest fluorescence quenching, therefore the effect of the position and number of the guanine bases in the overhang region was examined in greater detail. The number of guanine residues was found to be directly proportional to the degree of

Table 2
Fluorescence quantum yields of Alexa-488- and FAM-labelled probes upon hybridisation to various target oligonucleotides with and without 3′ overhang region, and with different overhang sequence

Target	Quantum yield (% quantum yield)	
	Alexa-488 labelled	FAM-labelled
Probe	0.556 (83.8)	0.428 (55.7)
No-overhang	0.664 (100)	0.767 (100)
TTGT	0.599 (90.2)	0.543 (70.8)
TGTT	0.612 (92.2)	0.561 (73.1)
GTTT	0.618 (93.0)	0.539 (70.2)
TTTG	0.610 (91.9)	0.573 (74.7)
GGTT	0.598 (90.1)	0.516 (67.2)
TGTG	0.497 (74.9)	0.428 (55.7)
GTGT	0.539 (81.2)	0.459 (59.8)
TTGG	0.541 (81.6)	0.465 (60.6)
GGGT	0.487 (73.3)	0.406 (52.9)
TGGG	0.464 (69.9)	0.384 (50.0)
AAAA	0.551 (86.9)	0.665 (86.8)
CCCC	0.699 (105.3)	0.666 (86.7)
TTTT	0.711 (107.2)	0.612 (80.3)
GGGG	0.437 (65.8)	0.329 (42.9)

The quantum yield data was obtained via comparison with a fluorescein standard with known quantum yield under specified conditions. Quantum yield data was derived as described in Material and methods. The data shown is the average quantum yield value generated from five independent hybridisation reactions, where each spectrum was recorded in duplicate. For each complex, standard error of the mean (S.E.M.) was typically <5% of the total value. The values in brackets refer to quantum yield percentage relative to that of the hybridisation reaction employing the no-overhang target that was set to 100.

fluorescence quenching for both probes, with four guanine bases generating the most quenching. The position of the guanine in the overhang sequence appeared not important for both FAM and Alexa-488 fluorescence when a single guanine was present. Though the GGTT sequence for both Alexa-488 and FAM appeared to cause reduced quenching levels compared to other sequences containing two guanine bases. Upon hybridisation of the probe to its complementary sequence with no-overhang target, an increase in fluorescence was observed for both Alexa-488- and FAM-labelled probes. It is apparent that duplex formation inhibits interstrand fluorescence quenching for both fluorophores.

3.2. Temperature dependence of fluorescent quenching

Changes in fluorescence upon hybridisation were also analysed in real-time using a thermal cycler with a fluorescent detector (LightCycler, Roche). Employing a temperature gradient from 30 to 95 °C, the fluorescence of the reverse reaction (melting of the hybridisation products) could be analysed. At the concentration of probe and target employed (100 and 150 nM, respectively) it was assumed that in the unhybridised state collisional/dynamic quenching of the probe from guanine residues on the target oligo would not be significant. The melting temperature (T_m) of the duplexes between various targets and probes was below 65 °C; therefore, at 95 °C, all the samples would be in the unhybridised state and the fluorescence intensity should be equal among all samples with the same concentration of the probe. All the lightcycler data was therefore normalized at 95 °C [5]. Data was compared to the fluorescence of the hybridisation reaction with the no-overhang target. The fluorescence from a series of hybridisation experiments is shown in Fig. 1 as a function of the temperature. Generally, as the temperature increases, the fluorescence quantum yield decreases due to enhanced nonradiative depopulation of the excited state of the fluorophore.

When the lightcycler data was compared to the steady-state fluorescence data a linear correlation between the two methods was observed, generating R^2 values of 0.972 and 0.977 for the Alexa-488 and FAM data, respectively (Fig. 1). It is apparent that the data derived from the steady-state measurements mirror that obtained by a thermal cycler used for real-time PCR experiments.

We examined the T_m values of those hybridisation reactions that showed a large change in fluorescence intensity between the hybridised and unhybridised states. No correlation between the overhang sequence and melting temperature could be obtained, other than duplexes with no-overhang target typically displayed a consistent ~1.6 °C higher T_m than those with the 3′ 4-base overhang targets (data not shown). The average melting temperatures for duplexes with the overhang region were 62.3 °C (SD, 1.9) for Alexa-488 probe and 62.0 °C (SD, 2.0) for FAM probe,

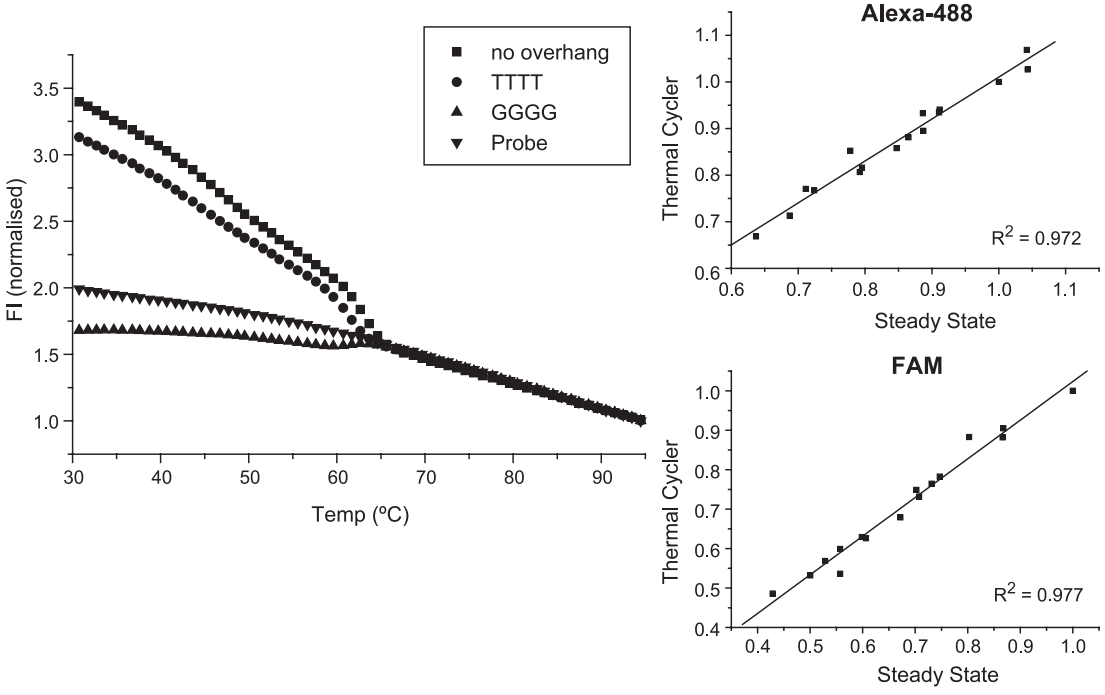

Fig. 1. Real-time monitoring of the melting of DNA duplexes. Shown are the melting curves for three FAM-labelled DNA duplexes each with a unique 3′ overhang sequence of four homogeneous bases (●: TTTT, ▲: GGGG and ■: no overhang) and the single-stranded FAM-labelled probe (▼) as a control. Thermal cycler data was normalized at 95 °C and fluorescence intensity was measured at 30 °C. The two inserts (upper for Alexa-488, lower for FAM) detail the linear relationship between the thermal cycler data (the average value generated from four independent reactions, S.D. values were <5% of total signal) and steady-state fluorescence data (Table 2), for all the duplexes detailed in Table 1. The steady-state data were calculated in terms of quantum yield, whereas the LightCycler data were shown in arbitrary fluorescence intensity units. Both data sets were expressed in relation to the fluorescence intensity/quantum yield values obtained with the duplex with no-overhang target.

respectively, which is somewhat below the theoretical prediction of 65 °C.

3.3. Fluorescence anisotropy (r) of the hybridised complexes

The mechanism of fluorescence quenching of FAM through guanine nucleotides is thought to involve a photon-induced electron transfer mechanism [7], facilitated by the close association of the two species. Fluorescence anisotropy data can be used to determine possible interactions between the fluorophore and its microenvironment through changes in the dye mobility [18,19]. We therefore analysed the fluorescence anisotropy from a series of probe/target hybridisation reactions to see if there was any relationship between quantum yield and mobility of the fluorophore in the complexes with various 3′ overhangs. A correlation between anisotropy and quantum yield was observed, generating R^2 values of 0.641 and 0.454 for Alexa-488 and FAM fluorophores, respectively (Fig. 2). For both Alexa-488 and FAM probes, the hybridisation reaction with the no-overhang target displayed relatively high anisotropy values. This is surprising in that with no adjacent 3′ overhang region, the fluorophore should display a large rotational freedom and hence a relatively low anisotropy compared to those oligos with 3′ overhangs. The potential mechanisms for the enhanced anisotropy displayed by duplexes with no 3′ overhang are detailed in the Discussion section.

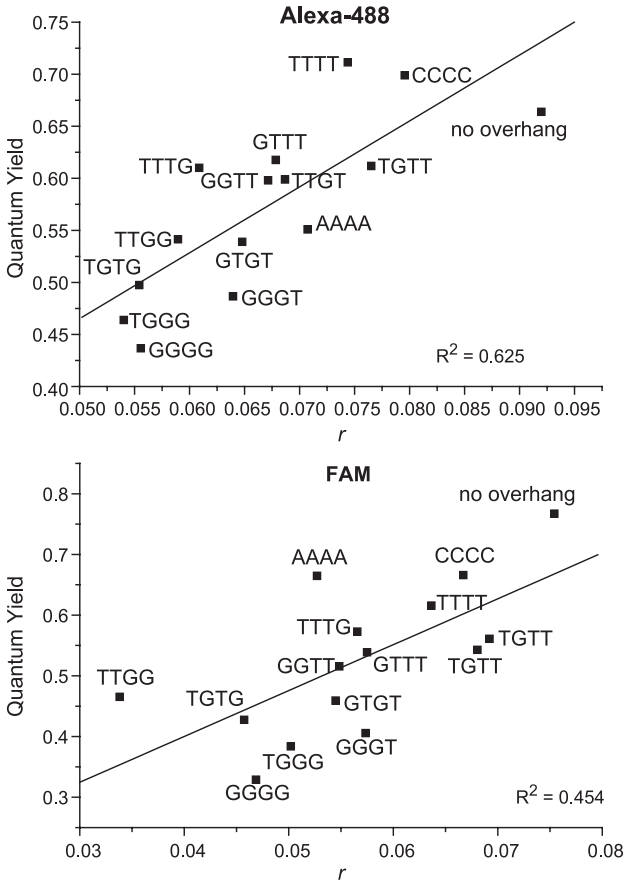

Fig. 2. The relationship between fluorescence quantum yield and anisotropy for the hybridisation reactions employing Alexa-488- and FAM-labelled probes. Quantum yield data was obtained as described in Table 2. The anisotropy data was measured as described in the Material and Methods. The anisotropy data for each hybridised oligo shown is mostly the average from two independent reactions (four repeats for the TTTT, TTTG, and GGGG incorporated duplexes), where each spectra was recorded in duplicate, generating S.E.M. values of typically <10% of the total *r*-value.

4. Discussion

Work by Nazarenko et al. [5] found that fluorescence quenching of fluorescein that was attached next to 3′ end of the probe oligonucleotide by a 5′ 1–2 guanine base overhang on the complementary target strand was less than by a terminal G–C pair, although the magnitude of quenching was still significant. Comparison with other reported data is problematic due to the differences in oligonucleotide sequence and furthermore because the data is often not quantitative; that is, it is expressed relative to the single-stranded probe. We have therefore chosen to express our data relative to the fluorescein standard (SRM 1932) with a known quantum yield. Previously, many authors described a decrease in fluorescence upon hybridisation [4–6], which was attributed to quenching from a guanine base in the complementary strand, often adjacent to the fluorophore-labelled base (cytosine). The present study employing the hybridisation reaction of the probe to the no-overhang target displayed the opposite effect with a large increase in intensity occurring upon hybridisation (Table 2). When the probe was in the unhybridised state, we inferred that the reduced rigidity of the oligonucleotide would allow the fluorophore to interact with any of the guanine bases within the probe. This could result in the lower quantum yield of the probe (FAM: 0.428) compared to the duplex with the complementary strand (0.767). We have observed similar quantum yield changes for a different FAM-labelled probe hybridised to its complementary strand (from 0.52 to 0.7 upon hybridisation) [19]. Although the C6 aminoalkyl linker of the fluorophore allows an interaction with approximately the first 5 bp next to the label, the guanine bases on the complementary strand doesn't appear to quench the fluorescence of FAM on the probe sequence.

Both Alexa-488- and FAM-labelled probes displayed guanine-base-sensitive fluorescence (Table 2). FAM-labelled probes appeared to be more sensitive to the presence of guanine bases compared to Alexa-488 and the difference could be due to the reduction potentials of the respective dyes [6]. For both dyes the degree of quenching observed is proportional to the number of guanine bases in the overhang region. For the FAM-labelled probe, the targets containing 3–4 guanine bases in the overhang region quenched up to 50% of the fluorescence of the duplex without an overhang. The magnitude of the decrease would

lead to lower signal to background ratios for intensity derived data, especially applications employing the dye as an acceptor of energy transfer. When designing real-time PCR assays, probes with multiple guanine bases on the complementary strand should be avoided, both in the complementary region and the overhang region adjacent to the fluorophore.

The data derived from both the Alexa-488- and FAM-labelled probes indicate that only guanine base in the 3′ overhang causes significant fluorescence quenching (Table 2). The position of the guanine in the 4-base overhang region appears not important given that all four overhang targets containing a single guanine base exhibit similar fluorescence quantum yields (Table 2). This suggests that the C6 linker attached to both dyes confers a high degree of mobility to the fluorophore facilitating its interaction with any of the bases in the overhang region. It is possible that 1–2 bases in the overhang sequence beyond the current 4-base positions in the target might also cause fluorescence quenching in some degree. Hence, further studies are required to determine the extent of this effect.

The apparent quenching of Alexa-488 by adenine bases ('AAAA' in Table 2) regarding to 'CCCC' and 'TTTT' overhangs and no-overhang duplexes appears novel. Torimura et al. [6] have reported that FAM could be quenched by adenosine monophosphate, though no data was presented for oligonucleotides containing adenine bases and Alexa-488 fluorophore to show such effect. It would be interesting to see if overhangs composed of mixed purines would produce an additive effect to the quenching of the Alexa-488 dye.

The quenching studies were also carried out using a thermal cycler to validate the steady-state data. A linear correlation between the two data sets was observed for both dyes (Fig. 1), suggesting the steady-state data is applicable to real-time PCR techniques. The changes in fluorescence intensity during the melting process of the duplexes allowed the determination of T_m values of the duplexes that displayed a large difference in quantum efficiency from the single-stranded probe. However, due to the smaller changes in fluorescence observed upon melting of the duplexes the standard deviations associated with T_m determination were close to 2 °C. Essentially no correlation between quantum yield and T_m could be established. On the other hand, the duplexes that contained no-overhang sequence consistently displayed a consistent 1.6 °C higher melting temperature than the duplexes with the overhang regions listed in Table 1. This enhanced stability with two no-overhang duplexes is very interesting and somewhat unexpected.

We further obtained the anisotropy data for both Alexa-488 and FAM labelled duplexes, which showed a correlation with fluorescence quantum yield (Fig. 2). Initially, we hypothesized that any potential interaction between the fluorophore and the quencher, guanosine base, would result in decreased rotational freedom of the dye and hence a larger anisotropy value. Nazarenko et al. [5] reported that for a 5′ -labelled fluorescein oligonucleotide, fluorescence intensity decreased and the polarization increased upon hybridisation with its complementary strand. This effect was attributed to quenching of the fluorophore by the terminal G–C base pair. In our earlier study [19], we also observed for 5′-labelled TAMRA oligonucleotide that fluorescence quenching was accompanied by the increase in polarization and melting temperature upon formation of the duplex with the long complementary strand. However, a quantitative comparison between these data sets is impossible due to the different oligonucleotide sequences employed and the presence of the short 3′ overhang region used in the present study.

Decreased mobility of the fluorophore was observed for both dyes in hybridisation reactions employing complementary sequence with no-overhang when compared to the oligonucleotides with 3′ overhang containing at least a single guanine base (Fig. 2). The result suggests that the position of the fluorophore is constrained by the formation of no-overhang duplex. A stacking interaction between the top of a DNA helix (C–G base pair) and a 5′ -labelled Cy3 dye was reported by Norman et al. [18], resulting in limited mobility of the dye with a relatively large anisotropy value of ~0.3. Although Alexa-488 and FAM fluorophores bear more negative charges than Cy3 dye molecule, the stacking interaction may still be possible given that the T_m of the no-overhang duplex is 1.6 °C higher than that of duplexes with a 3′ overhang and the quantum yield of the no-overhang duplex is also higher than those with at least one guanine base in the overhang region. The presence of a single guanine appears to interfere with the relatively weak stacking interaction, resulting in higher mobility and lower quantum yield of the fluorophore. Another possibility is that the interaction between the fluorophore and the guanine residue adjacent to the fluorophore-labelled nucleotide (Thymine) results in more rigidity of the fluorophore in the absence of the overhang. Since the quantum yield of the no-overhang duplex labelled with FAM (0.767 in Table 2) is close to that of dT-FAM (0.810, unpublished result), this possibility is less likely given that close proximity of FAM and guanine will cause fluorescence quenching of FAM.

We used Amber molecular mechanics (MM) described earlier to model the possible structures of the hybridisation products. Fig. 3a shows the optimised geometry for one likely configuration of Alexa-488 at the end of the duplex for the case of no overhang. There is a specific interaction between the carboxyl oxygen of Alexa-488 and the NH_2 group on the adenine base in the complementary strand illustrated by the green circle. Fig. 3b shows the optimised geometry of a configuration of Alexa-488 in the duplex with a TGTT overhang. There is considerable deviation from an ideal duplex structure at the point of attachment. The geometry was optimised for all overhang sequences shown in Table 1. The total binding energy for each optimised geometry increased with the increase in the

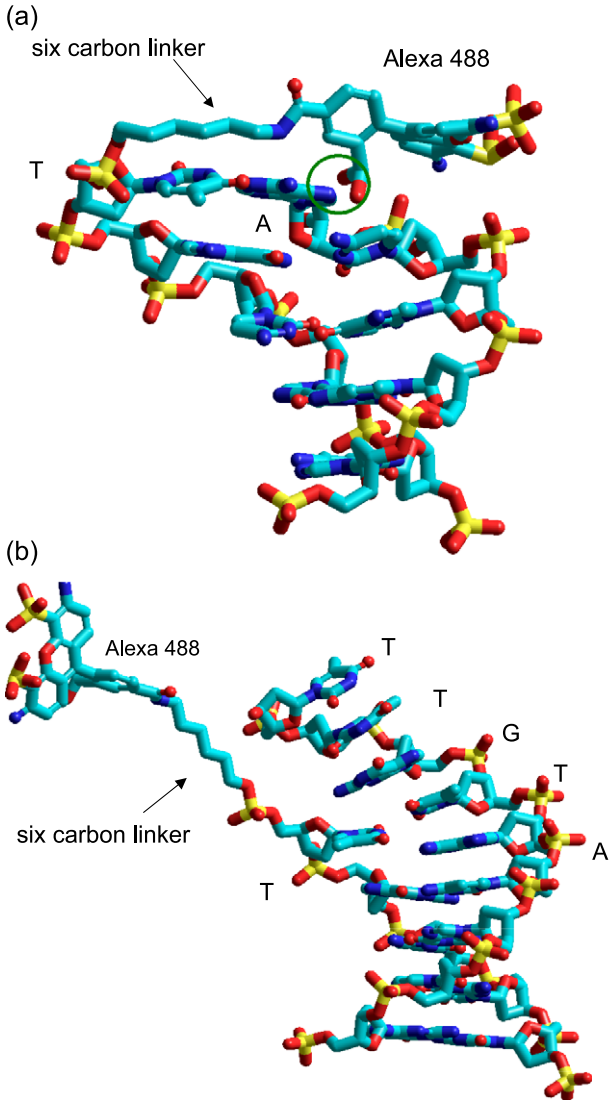

Fig. 3. Duplex structures predicted by using Amber molecular mechanics (MM) combined with AM1 semiempirical calculation. (a) The optimised geometry for the duplex formed between Alexa-488-labelled probe and no-overhang target. The model predicts a specific interaction between the carboxyl oxygen on Alexa-488 and NH_2 group on the A base of the target illustrated by the green circle. (b) A likely configuration of the duplex formed between Alexa-488-labelled probe and the target with a TGTT overhang. Only the first five base pairs of the duplex were chosen for the model computation, and were sufficient to preserve the double-helical structure of the duplex upon attachment of Alexa-488 fluorophore and the overhang. Hydrogen atoms are not shown for simplification purpose.

number of G bases in the overhang region. We further calculated the binding energy of the duplex with the overhang region but in the absence of Alexa-488 fluorophore (replacing Alexa-488 with a hydrogen atom). The difference in binding energy with and without Alexa-488 decreased with the number of G bases. Thus, the contribution of Alexa-488 to the overall binding decreased with the number of G bases, and may provide an explanation for the decrease in anisotropy of Alexa-488 fluorophore with the increase in the number of G bases in the overhang region shown in Fig. 2.

The time-resolved data from the literature shows that where fluorescein quenching via guanine bases occurred, a decrease in the magnitude of the longer-time component (4.2 ns) and an increase in the magnitude of the shorter-time components (0.5 and 2.7 ns) was observed [4]. Similar results were also obtained for the rhodamine-labelled oligos, where guanine base induced fluorescence quenching was attributed to a decrease in the fluorescence lifetime of the dye molecule [20,21]. The change to shorter lifetimes may be characteristic of guanine quenching, resulting in increased anisotropy values of the dye molecules since more polarized light would be emitted during the shorter lifetime, as described by the Perrin equation [22]. The opposite correlation was observed in the present study, with guanine containing overhangs generating lower anisotropy values, and therefore the Perrin equation cannot be simply applied to explain the changes in anisotropy for the fluorophores observed in Fig. 2. On the other hand, our molecular mechanics model shows that the presence of the 3′ overhang may make stacking interaction between fluorophore and the end of helix in the case of no-overhang duplex impossible. The stacking interaction could result in higher polarization of the fluorophores observed for duplexes without the overhang. The dynamic quenching by guanine base in the 3′ overhang region likely prohibits specific interaction between the fluorophore and the single guanine base in the presence of several such bases as shown by the model calculation that the binding of Alexa-488 to the overhang region decreases with the number of G bases. Rationally, double-stranded DNA molecules are likely to move in complex ways and maintain equilibrium between various conformations.

Acknowledgements

We wish to thank Joe Blasic and Margaret Kline for their help with running and analysing the DNA gels. This work was supported by the Glazebrook Fellowship (J.E. Noble), which was issued by the Department of Trade and Industry (UK) supporting scheme that promotes collaborations among National Measurement Institutes.

References

[1] Y. Xiao, P.E. Barker, Semiconductor nanocrystal probes for human metaphase chromosomes, Nucleic Acids Res. 32 (2004) e28.
[2] D. Shalon, S.J. Smith, P.O. Brown, A DNA microarray system for analyzing complex DNA samples using two-color fluorescent probe hybridization, Genome Res. 6 (1996) 639–645.
[3] C.A. Heid, J. Stevens, K.J. Livak, P.M. Williams, Real time quantitative PCR, Genome Res. 6 (1996) 986–994.
[4] S.P. Lee, D. Porter, J.G. Chirikjian, J.R. Knutson, M.K. Han, Fluorometric assay for DNA cleavage reactions characterized with *Bam*HI restriction-endonuclease, Anal. Biochem. 220 (1994) 377–383.
[5] I. Nazarenko, R. Pires, B. Lowe, M. Obaidy, A. Rashtchian, Effect of primary and secondary structure of oligodeoxyribonucleotides on the

fluorescent properties of conjugated dyes, Nucleic Acids Res. 30 (2002) 2089–2095.
[6] M. Torimura, S. Kurata, K. Yamada, T. Yokomaku, Y. Kamagata, T. Kanagawa, R. Kurane, Fluorescence-quenching phenomenon by photoinduced electron transfer between a fluorescent dye and a nucleotide base, Anal. Sci. 17 (2001) 155–160.
[7] C.A.M. Seidel, A. Schulz, M.H.M. Sauer, Nucleobase-specific quenching of fluorescent dyes: 1. Nucleobase one-electron redox potentials and their correlation with static and dynamic quenching efficiencies, J. Phys. Chem. 100 (1996) 5541–5553.
[8] H. Sigmund, T. Maier, W. Pfleiderer, A new type of fluorescence labeling of nucleosides, nucleotides and oligonucleotides, Nucleosides Nucleotides 16 (1997) 685–696.
[9] J.P. Knemeyer, N. Marme, M. Sauer, Probes for detection of specific DNA sequences at the single-molecule level, Anal. Chem. 72 (2000) 3717–3724.
[10] S. Kurata, T. Kanagawa, K. Yamada, M. Torimura, T. Yokomaku, Y. Kamagata, R. Kurane, Fluorescent quenching-based quantitative detection of specific DNA/RNA using a BODIPY FL-labeled probe or primer, Nucleic Acids Res. 29 (2001) e34.
[11] S.R. Lewin, M. Vesanen, L. Kostrikis, A. Hurley, M. Duran, L. Zhang, D.D. Ho, M. Markowitz, Use of real-time PCR and molecular beacons to detect virus replication in human immunodeficiency virus type 1-infected individuals on prolonged effective antiretroviral therapy, J. Virol. 73 (1999) 6099–6103.
[12] A.O. Crockett, C.T. Wittwer, Fluorescein-labeled oligonucleotides for real-time PCR: using the inherent quenching of deoxyguanosine nucleotides, Anal. Biochem. 290 (2001) 89–97.
[13] M. Zuker, Mfold web server for nucleic acid folding and hybridization prediction, Nucleic Acids Res. 31 (2003) 3406–3415.
[14] J. Zhao, L.K. Tamm, FTIR and fluorescence studies of interactions of synaptic fusion proteins in polymer-supported bilayers, Langmuir 19 (2003) 1838–1846.
[15] N. Klonis, A.H.A. Clayton, E.W. Voss, W.H. Sawyer, Spectral properties of fluorescein in solvent–water mixtures: applications as a probe of hydrogen bonding environments in biological systems, Photochem. Photobiol. 67 (1998) 500–510.
[16] G.K. Turner, An absolute spectrofluorimeter, Science 146 (1964) 183–189.
[17] T.E. Cheatham III, M.A. Young, Molecular dynamics simulation of nucleic acids: successes, limitations, and promise, Biopolymers (Nucleic Acid Sci.) 56 (2001) 232–256.
[18] D.G. Norman, R.J. Grainger, D. Uhrin, D.M.J. Lilley, Location of cyanine-3 on double-stranded DNA: importance for fluorescence resonance energy transfer studies, Biochemistry 39 (2000) 6317–6324.
[19] L. Wang, A.K. Gaigalas, J. Blasic, M.J. Marcia, Spectroscopic characterization of fluorescein- and tetramethylrhodamine-labeled oligonucleotides and their complexes with a DNA template, Spectrachim. Acta, Part A 60 (2004) 2741–2750.
[20] L. Edman, U. Mets, R. Rigler, Conformational transitions monitored for single molecules in solution, Proc. Natl. Acad. Sci. U. S. A. 93 (1996) 6710–6715.
[21] S. Wennmalm, L. Edman, R. Rigler, Conformational fluctuations in single DNA molecules, Proc. Natl. Acad. Sci. U. S. A. 94 (1997) 10641–10646.
[22] J.R. Lakowicz, Principles of Fluorescence Spectroscopy, 2nd ed., Kluwer Academic/Plenum Publishers, New York, 1999, pp. 303–306.